Journal of Theoretical Biology 572 (2023) 111587

Contents lists available at ScienceDirect

Journal of Theoretical Biology

journal homepage: www.elsevier.com/locate/yjtbi

Eco-evolutionary dynamics in finite network-structured populations with migration

Karan Pattni [a,*], Wajid Ali [a], Mark Broom [b], Kieran J. Sharkey [a]

[a] Department of Mathematical Sciences, University of Liverpool, United Kingdom
[b] Department of Mathematics, City, University of London, United Kingdom

ARTICLE INFO

Keywords:
Evolution
Eco-evolutionary dynamics
Fixation probability
Networks

ABSTRACT

We consider the effect of network structure on the evolution of a population. Models of this kind typically consider a population of fixed size and distribution. Here we consider eco-evolutionary dynamics where population size and distribution can change through birth, death and migration, all of which are separate processes. This allows complex interaction and migration behaviours that are dependent on competition. For migration, we assume that the response of individuals to competition is governed by tolerance to their group members, such that less tolerant individuals are more likely to move away due to competition. We look at the success of a mutant in the rare mutation limit for the complete, cycle and star networks. Unlike models with fixed population size and distribution, the distribution of the individuals per site is explicitly modelled by considering the dynamics of the population. This in turn determines the mutant appearance distribution for each network. Where a mutant appears impacts its success as it determines the competition it faces. For low and high migration rates the complete and cycle networks have similar mutant appearance distributions resulting in similar success levels for an invading mutant. A higher migration rate in the star network is detrimental for mutant success because migration results in a crowded central site where a mutant is more likely to appear.

1. Introduction

Migration is one of the drivers of evolutionary processes. One of the ways in which the effect of migration can be captured is to consider a subdivided population. Each subdivision is a unit of space that can be occupied by one or many individuals. In ecology such models are used to study species in fragmented habitats (Hanski, 1998) such as the fritillary butterfly (Wahlberg et al., 2002). In evolutionary game theory this enables modelling interactions between subsets of individuals (Broom and Rychtář, 2012). Individuals can either migrate freely between these sites as in the classical island model (Wright, 1943), or can be restricted to geographically adjacent sites as in the stepping stone model (Kimura and Weiss, 1964). From a population genetics perspective, such models are used to study the effect of population subdivision on the fixation of a mutant type in a resident population. Maruyama (1970, 1974) showed that for certain assumptions the fixation probability is independent of the population subdivision. In this model, each subdivision is of infinite size. Evolutionary graph theory (EGT) (Lieberman et al., 2005) theoretically restricts migration using networks. Network structure was shown to affect the evolutionary dynamics by amplifying or suppressing the fixation probability of a mutant (Lieberman et al., 2005; Broom and Rychtář, 2008; Hadjichrysanthou et al., 2011; Hindersin and Traulsen, 2015), and it also affects the time it takes to reach fixation (Frean et al., 2013; Hindersin and Traulsen, 2014; Tkadlec et al., 2019). In EGT, each subdivision has a fixed and finite size of one individual and, more recently, the case with subdivisions of size greater than 1 has been considered (Yagoobi and Traulsen, 2021). Our objective is to construct an ecologically relevant model that allows us to consider the case where subdivisions have variable and finite size.

Migration in EGT occurs through replacement events where birth, death and migration are all combined such that an offspring replaces an individual in an adjacent site. Birth, death and migration can be combined to give different replacement dynamics (Shakarian et al., 2012). Ecologically relevant dynamics can be obtained by considering non-replacement dynamics where birth and death are decoupled allowing for variable population size. The individual-based model of Champagnat et al. (2006) is an example of this, where the time-scale of individual level processes can be changed to consider different types of evolutionary models. For example, the evolution of RNA viruses (Grenfell et al., 2004) where evolutionary and ecological timescales overlap. In Pattni et al. (2021) network structure was incorporated into the

* Corresponding author.
E-mail address: karanp@liverpool.ac.uk (K. Pattni).

https://doi.org/10.1016/j.jtbi.2023.111587
Received 10 February 2023; Received in revised form 6 July 2023; Accepted 20 July 2023
Available online 28 July 2023

Table 1
Summary: Notations for framework, and their definitions and descriptions.

Notation	Definition	Description
N	≥ 1	Number of distinct sites.
W	$W_{m,n} \geq 0$	Weighted $N \times N$ matrix representing network of sites.
$\mathcal{U}$	$\subset \mathbb{R}^l$	l real-valued phenotypic traits of an individual.
$\mathcal{X}$	$= \{1, \dots, N\}$	Set of sites an individuals can occupy.
i	$= (U_i, X_i)$ for $U_i \in \mathcal{U}$ and $X_i \in \mathcal{X}$	The traits of an individual.
I_i		An individual with traits i.
$\mathcal{S}$	$= \{i^{m(i)} : i \in \mathcal{I}, \mathcal{I} \subseteq \mathcal{U} \times \mathcal{X}\}$	Multiset that gives the state of the population, where $m : \mathcal{I} \to \mathbb{Z}^+$ is the multiplicity (number of occurrences) of i.
$\mathcal{S}_n$	$= \{i \in \mathcal{S} : X_i = n\}$	Individuals present in site n, therefore, $\mathcal{S}_n \subseteq \mathcal{S}$.
$d(i, \mathcal{S})$	≥ 0	Death rate of I_i in state $\mathcal{S}$.
$b(i, \mathcal{S})$	≥ 0	Birth rate of I_i in state $\mathcal{S}$.
$\mu(i)$	≥ 0	Probability that an offspring of I_i carries a mutation.
$M(u, v)$	≥ 0	Probability that offspring has mutated trait v when parent has trait u.
$m(i, x, \mathcal{S})$	≥ 0	Migration rate of I_i to site x in state $\mathcal{S}$.
ϕ	$: \mathcal{S} \to \mathbb{R}$	Real-valued bounded function that acts on the state of the system.
$\mathcal{L}$		Markov process generator, it describes how the expected value of ϕ changes for an infinitesimal time interval.
$h_{\mathcal{A}}(\mathcal{S})$	$\in [0, 1]$	Probability of starting in state $\mathcal{S}$ and hitting state in set $\mathcal{A}$.

model of Champagnat et al. (2006) such that death is separate but birth and migration are coupled. Using this model it was shown that most EGT replacement dynamics can be obtained in limiting cases. This shows that replacement dynamics models represent special cases of models with non-replacement dynamics. For those replacement dynamics that could not be obtained, it suggests that a different kind of non-replacement dynamics may be required. The next logical step, which we consider in this paper, is a model where death, birth and migration are all uncoupled.

Depending upon how migration is defined allows us to consider different ecological processes. When migration is coupled with birth, this is akin to dispersal in plants (Fournier and Méléard, 2004) or the spread of infection (Rosenquist, 2010). Uncoupled migration, where individuals can freely move between sites, allows us to consider complex behaviours such as animal migration (Bauer and Klaassen, 2013). It also enables the study of social dilemmas (Santos et al., 2006; Broom et al., 2019) where assortment or grouping is required to achieve a social outcome (Fletcher and Doebeli, 2009). Density-dependent migration is one way of capturing this kind of migratory behaviour as it explains a wide variety of ecological aggregations (Liu et al., 2016). From a mathematical perspective, various complex migration behaviours can be constructed that can depend upon the history of individuals (Broom and Rychtář, 2012; Kölzsch et al., 2018). In this paper we consider an example of migration behaviour that is dependent upon the tolerance to other individuals, such that for low group tolerance individuals prefer being alone.

We start by explaining the framework in Section 2, where the rare mutation limit evolutionary scenario is described. In Section 3 we provide an example of a birth–death-migration model derived from the framework. We consider the trivial case with one site, the low migration limit and a general migration rate. For the general migration rate we investigate the effect of migration rate and how this compares to the low migration limit.

2. Modelling framework

A general description of the modelling framework used that is based on the model of Champagnat et al. (2006) is given (see Table 1 for summary of notation). In this model individuals have a continuous number of traits and reproduce asexually. In Pattni et al. (2021) network structure was incorporated into this model such that individuals in the population are spread over a fixed network of distinct but connected sites that can have no, one or many individuals at a given time. The modelling framework here is updated so that migration is a separate event from birth and death. The population can now change in four distinct ways: birth without mutation, birth with mutation, death and migration. The population size and composition can change due to birth and death, whereas the distribution of individuals across the network of sites can change due to birth, death and migration.

The framework allows modelling the evolution of multiple traits. It therefore describes what is the current composition of the population in terms of these different traits. As individuals can move between different sites, the composition of different traits in each site need to be accounted for. This is described mathematically as follows. Individuals can have l real-valued traits contained within the set $\mathcal{U} \subset \mathbb{R}^l$. The sites that individuals can occupy is given by set $\mathcal{X} = \{1, \dots, N\}$. The characteristics of an individual are given by $i = (U_i, X_i)$, where $U_i \in \mathcal{U}$ and $X_i \in \mathcal{X}$. An individual with characteristics i is denoted by I_i. The state of the population is given by a multi-set $\mathcal{S}$, which means that for each individual with characteristics i there is a copy of i in $\mathcal{S}$. Formally we write this as $\{i^{m(i)} : i \in \mathcal{I}, \mathcal{I} \subseteq \mathcal{U} \times \mathcal{X}\}$ where $m : \mathcal{I} \to \mathbb{Z}^+$ is the multiplicity (number of occurrences) of i. Individuals in the same site are given by set $\mathcal{S}_n = \{i \in \mathcal{S} : X_i = n\}$.

The framework specifies how the different sites are connected to each other allowing individuals to move between them. It accounts for the direction of migration between sites and also the likelihood of migration between sites. Formally this is described as follows. The connections between sites are given by a directed and weighted network represented by a matrix W with entries $W_{m,n} \geq 0$. An individual can move from site m to n if site m is connected to site n; that is, $W_{m,n} > 0$.

In the framework the state of the population can change through birth, death and migration. All these processes are separate and independent of each other. In the case of birth it specifies whether a mutation occurs and what kind of mutation the offspring carries. For migration, it needs to specify where an individual migrates to depending upon its current position. Mathematically these processes are described as follows. Individuals are assumed to reproduce asexually such that they place their offspring on the same site. The rate at which individual I_i gives birth is given by $b(i, \mathcal{S}, W)$. If there is no mutation, the offspring of individual I_i has characteristics $i = (U_i, X_i)$. With probability $\mu(i)$, individual I_i gives birth to an offspring with mutation. In this case, the probability that I_i gives birth to an offspring with trait u is $M(U_i, u)$ such that all mutations are contained within $\mathcal{U}$, that is, $M(U_i, u) = 0$ if $u \notin \mathcal{U}$. The rate at which individual I_i dies is given by $d(i, \mathcal{S}, W)$. The rate at which individual I_i migrates to site x is given by $m(i, x, \mathcal{S}, W)$. Since the network structure W is assumed to be fixed, we use $b(i, \mathcal{S})$, $d(i, \mathcal{S})$ and $m(i, x, \mathcal{S})$ for the birth, death and migration rate respectively.

Finally, the processes of birth, death and migration need to be put together to describe how the state of the population changes over time. One way to think about this is that there are separate clocks counting down each of these processes. If, for example, the clock for death

reaches zero first, the population is updated through a death event. The clocks then reset and the process carries on. Mathematically, the framework describes the evolution of the population using a continuous time Markov process. The generator $\mathcal{L}$ that acts on real bounded functions $\phi(\mathcal{S})$ that describes the infinitesimal dynamics of the state of the population at time t is given by

$$\begin{aligned}\mathcal{L}\phi(\mathcal{S}) = &\sum_{i\in\mathcal{S}}[1-\mu(i)]b(i,\mathcal{S})[\phi(\mathcal{S}\cup\{i\})-\phi(\mathcal{S})]\\ &+\sum_{i\in\mathcal{S}}\mu(i)b(i,\mathcal{S})\int_{\mathbb{R}^l}[\phi(\mathcal{S}\cup\{(u,X_i)\})-\phi(\mathcal{S})]M(U_i,u)du\\ &+\sum_{i\in\mathcal{S}}d(i,\mathcal{S})[\phi(\mathcal{S}\backslash\{i\})-\phi(\mathcal{S})]\\ &+\sum_{i\in\mathcal{S}}\sum_{x\in\mathcal{X}}m(i,x,\mathcal{S})[\phi(\mathcal{S}\cup\{(U_i,x)\}\backslash\{i\})-\phi(\mathcal{S})].\end{aligned} \tag{1}$$

The first line describes birth without mutation, the second line describes birth with mutation, the third line describes death and the fourth line describes migration.

Now that we know how the evolution of the population is described, we want to be able to say what the expected behaviour is of this system. In particular, we are interested in the expectation of reaching a certain state of the system given the initial conditions. This is known as the hitting probability. Using the infinitesimal dynamics in Eq. (1), the probability $h_{\mathcal{A}}(\mathcal{S})$ of starting in state $\mathcal{S}$ and hitting a state in set $\mathcal{A}$ is calculated as follows

$$\mathcal{L}h_{\mathcal{A}}(\mathcal{S}) = 0 \tag{2}$$

with boundary condition $h_{\mathcal{A}}(\mathcal{S}) = 1$ for $\mathcal{S}\in\mathcal{A}$ (see Pattni et al. (2021), Appendix A).

2.1. Evolution in the rare mutation limit

The modelling framework can be used to construct models of varying complexity where different types of mutations can overlap with one another, that is, there is clonal interference. Models related to EGT typically assume no clonal interference and therefore, to enable comparisons with these models, we consider the rare mutation limit. In the rare mutation limit we assume that $\mu(i) = \mu \to 0\ \forall i$ so that the population evolves through adaptive sweeps (Gerrish and Lenski, 1998). This means that, prior to a mutation arising, the population is homogeneous with all individuals having the same traits. This is because, when a mutation appears, either all individuals with the mutation (referred to as mutants and denoted M) die out or all individuals without the mutation (referred to as residents and denoted R) die out prior to another mutation arising. There can therefore be at most two types in the population, a type R and a type M. Let $\mathcal{U} = \{R, M\}$, then the set of states where all individuals are residents is given by $\mathcal{R} = \{\mathcal{S} : U_i = R,\ \forall i\in\mathcal{S}\}$; similarly the set of all states with mutants is given by $\mathcal{M} = \{\mathcal{S} : U_i = M,\ \forall i\in\mathcal{S}\}$. The dynamics of the system can therefore be described without the mutation step; that is, Eq. (1) simplifies to

$$\begin{aligned}\mathcal{L}\phi(\mathcal{S}) = &\sum_{i\in\mathcal{S}}b(i,\mathcal{S})[\phi(\mathcal{S}\cup\{i\})-\phi(\mathcal{S})]\\ &+\sum_{i\in\mathcal{S}}d(i,\mathcal{S})[\phi(\mathcal{S}\backslash\{i\})-\phi(\mathcal{S})]\\ &+\sum_{i\in\mathcal{S}}\sum_{x\in\mathcal{X}}m(i,x,\mathcal{S})[\phi(\mathcal{S}\cup\{(U_i,x)\}\backslash\{i\})-\phi(\mathcal{S})].\end{aligned} \tag{3}$$

When the population is in a homogeneous state with all residents prior to a mutant arising, i.e. $\mathcal{S}\in\mathcal{R}$, we are interested in determining the state in which a mutant appears. Let $\pi(\mathcal{S})$ be the probability that the population is in state $\mathcal{S}$. This can be calculated using Eq. (3) as follows

$$\mathcal{L}\pi(\mathcal{S}) = 0, \quad \mathcal{S}\in\mathcal{R} \tag{4}$$

with normalising condition

$$1 = \sum_{\mathcal{S}\in\mathcal{R}}\pi(\mathcal{S}). \tag{5}$$

The probability $p_{x,\mathcal{S}}$ that a mutant appears in site x in state $\mathcal{S}$ is proportional to the number of individuals in site x; that is,

$$p_{x,\mathcal{S}} = \frac{|\mathcal{S}_x|}{|\mathcal{S}|}\pi(\mathcal{S}). \tag{6}$$

Note that whether a unique solution to $\pi(\mathcal{S})$ exists depends upon the definition of birth, death and migration.

Once a mutation arises, the type that remains is said to have fixated in the population, and we are interested in the probability of mutants fixating. This is calculated by solving the hitting probability using Eq. (3) as follows

$$\mathcal{L}h_{\mathcal{M}}(\mathcal{S}) = 0 \tag{7}$$

with boundary conditions $h_{\mathcal{M}}(\mathcal{S}) = 1$ for $\mathcal{S}\in\mathcal{M}$ and $h_{\mathcal{M}}(\mathcal{S}) = 0$ for $\mathcal{S}\in\mathcal{R}$. To be precise with terminology, we refer to the fixation probability as the probability of one initial mutant fixating. Since there are multiple states with one mutant, we calculate the average fixation probability as follows

$$\rho = \sum_{\mathcal{S}\in\mathcal{R}}\sum_{x\in\mathcal{X}}p_{x,\mathcal{S}}h_{\mathcal{M}}(\mathcal{S}\cup\{(M,x)\}) \tag{8}$$

where $p_{x,\mathcal{S}}$ is the mutant appearance distribution, i.e. the probability that a mutant appears in site x when the population is in state $\mathcal{S}$.

3. Birth–death-migration model

To apply the modelling framework, we consider a birth–death-migration model that we can use to calculate the fixation probability. The birth rate is considered to be fixed and depends only on the type of individual:

$$b(i,\mathcal{S}) = \beta_{U_i}. \tag{9}$$

The death rate is given by

$$d(i,\mathcal{S}) = \delta_{U_i} + \sum_{j\in\mathcal{S}_{X_i}\backslash\{i\}}\gamma_{U_i,U_j} \tag{10}$$

where δ_u is the natural death rate of a type u individual and $\gamma_{u,v}$ is the death rate of a type u individual when competing with a type v individual.

We assume that individuals move with migration rate $\lambda > 0$. Where they move to will depend upon the structure of the network given by W. We assume that $W_{x,x} = 0$ and $\sum_{y\in\mathcal{X}}W_{x,y} = 1\ \forall x\in\mathcal{X}$; that is, all diagonal elements of W are zero and W is right-stochastic. This means that $W_{x,y}$ is the probability of migrating from site x to y. It is assumed that the networks are strongly connected so that every site is reachable from every other site. This means that individuals can migrate throughout the network ensuring that all states of the system can be obtained. In terms of fixation, this ensures that it is possible for a mutant to fixate in the population.

One way to determine the migration of individuals is to use positive density-dependent migration where the rate of migration increases with the number of individuals due to exploitation and interference (Bowler and Benton, 2005). We consider an extreme version of this where individuals have low group tolerance (LGT) such that they will migrate when in a group but stay when they are alone. This is defined as follows,

$$m^{\mathrm{LGT}}(i,x,\mathcal{S}) = \begin{cases}\lambda W_{X_i,x} & |\mathcal{S}_{X_i}| > 1,\\ 0 & |\mathcal{S}_{X_i}| = 1.\end{cases} \tag{11}$$

For comparison, we consider the other extreme where individuals have high group tolerance (HGT) such that individuals are insensitive to the group they are in so they migrate regardless of being in a group or not. The migration rate in this case is given by,

$$m^{\mathrm{HGT}}(i,x,\mathcal{S}) = \lambda W_{X_i,x}. \tag{12}$$

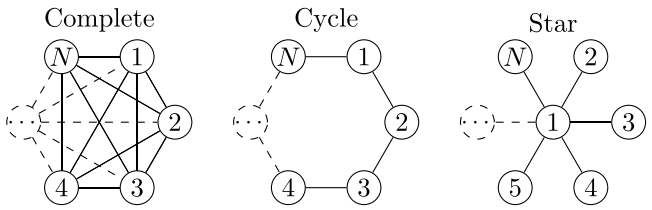

Fig. 1. Networks considered in this paper. Each node represents a site. N is the total number of sites. Each edge represents an incoming and outgoing weighted edge whose weights are given by W. Edges represent the permitted migration routes of individuals. In the star network site 1 is called the centre and sites 2 to N are called leaf sites.

3.1. Example of birth–death-migration model

As an initial application of the birth–death-migration model, we consider a simple example that enables us to obtain analytical results in certain limiting cases. The simplifications used are described as follows.

Different types of individuals differ in terms of their birth rate only and cannot die naturally. We set the birth rate of a resident to $\beta_R = 1$ and mutant to $\beta_M = 2$, unless specified otherwise. No natural death means that $\delta_u = 0$ for $u \in \{M, R\}$. This assumption is not part of the fundamental framework but specific to this example considered here. In particular, it is a convenient way of preventing a population from going extinct. An alternative way of dealing with extinction events is to reseed the population, however, we avoid this technicality. Individuals therefore die due to competition with an identical rate for all paired types, i.e. $\gamma_{u,v} = \gamma,\ \forall u, v$.

The complete ($W^{\bullet}$), cycle (W°) and star ($W^{\star}$) networks will be considered, they are illustrated in Fig. 1. For each network, $W^{\bullet}_{ii} = W^{\circ}_{ii} = W^{\star}_{ii} = 0\ \forall i \in \mathcal{X}$ and the non-zero weights are as follows

$$\left.\begin{aligned}
&\text{Complete: } W^{\bullet}_{ij} = 1/(N-1),\ i \neq j \text{ and } i, j \in \mathcal{X},\\
&\text{Cycle: } W^{\circ}_{i,i+1} = W^{\circ}_{j,j-1} = W^{\circ}_{1,N} = W^{\circ}_{N,1} = \tfrac{1}{2},\ i = 1, \dots, N-1 \text{ and } j = 2, \dots, N,\\
&\text{Star: } W^{\star}_{1,i} = \tfrac{1}{N-1},\ W^{\star}_{i,1} = 1,\ i = 2, \dots, N-1.
\end{aligned}\right\} \tag{13}$$

Due to the properties of the networks chosen, they will provide us with a base understanding of the birth–death-migration model without the need to run lengthy simulations across a wide range of networks. The complete network is the benchmark case where migration is possible between all sites. The complete and cycle networks have the property that the incoming and outgoing weights for each site are the same, i.e. $\sum_i W_{i,j} = \sum_j W_{j,i}\ \ \forall i, j \in \mathcal{X}$. This will allow us to compare the complete and cycle networks for similarities due to this property. On the other hand, the star network is an extreme example where a central site is connected to all other sites.

Details regarding the simulation of the birth–death-migration model example are given in the appendix. The simulations were carried out using the HTCondor distributed computing system (Thain et al., 2005).

3.2. Special case with single site

We first consider the case where there is one site. This will allow us to understand the intra-site dynamics. For the birth–death-migration model we can analytically calculate the stationary distribution of a homogeneous population (i.e. all residents or all mutants). Let $\pi^u_n = \mathbb{P}(S = \{(u, 1)^n\})$ be the probability that there are n individuals of type u in the population. Recall that the population cannot go extinct because we have assumed that the natural death rate is zero in this example (death only occurs by competition). The homogeneous population is therefore described by a reversible Markov process and we can obtain π^u_n using the detailed balance equations, which states that the transition rates do not change when time is reversed. In particular, the rate at which we transition from state n to $n-1$ due to a death event is the same as transitioning from state $n-1$ to n due to a birth event. In a state with n individuals each individual dies with rate $\gamma(n-1)$ and in a state with $n-1$ individuals each individual gives birth with rate β, so for $n \geq 2$ the detailed balance equations give

$$n\gamma(n-1)\pi^u_n = (n-1)\beta_u\pi^u_{n-1}$$

which simplifies to

$$\pi^u_n = \frac{1}{n}\frac{\beta_u}{\gamma}\pi^u_{n-1}$$

and through recursion we obtain

$$\pi^u_n = \frac{(\beta_u/\gamma)^{n-1}}{n!}\pi^u_1. \tag{14}$$

Using the fact that the stationary probabilities sum to 1 (i.e. $1 = \sum_{n=1}^{\infty}\pi_n$) and, setting $x = \beta_u/\gamma$ for brevity, we have that

$$1 = \sum_{n=1}^{\infty}\frac{x^{n-1}}{n!}\pi^u_1 = \frac{\pi^u_1}{x}\sum_{n=1}^{\infty}\frac{x^n}{n!} = \frac{\pi^u_1}{x}\left(-1 + \sum_{n=0}^{\infty}\frac{x^n}{n!}\right) = \frac{\pi^u_1}{x}\left(-1 + e^x\right),$$

which gives

$$\pi^u_1 = \frac{(\beta_u/\gamma)}{e^{\beta_u/\gamma} - 1}.$$

Substituting π^u_1 into Eq. (14) gives us the stationary probability,

$$\pi^u_n = \frac{(\beta_u/\gamma)^n}{n!}\frac{1}{e^{\beta_u/\gamma} - 1}.$$

Using the stationary probability we calculate the expected type u population size as follows

$$\sum_{n=1}^{\infty} n\pi^u_n = \frac{1}{e^{\beta_u/\gamma} - 1}\sum_{n=1}^{\infty} n\frac{(\beta_u/\gamma)^n}{n!} = \frac{(\beta_u/\gamma)e^{\beta_u/\gamma}}{e^{\beta_u/\gamma} - 1} = \frac{\beta_u/\gamma}{1 - e^{-\beta_u/\gamma}}.$$

The appearance of a mutant is proportional to the number of resident individuals in a given state. The probability that an initial mutant appears in a state with n residents is therefore given by

$$\mu^{\text{Init}}_n = \frac{n\pi^u_n}{\sum_{i=1}^{\infty} i\pi^u_i} = n\frac{(\beta_R/\gamma)^n}{n!}\frac{1}{e^{\beta_R/\gamma} - 1}\Big/\frac{(\beta_R/\gamma)e^{\beta_R/\gamma}}{e^{\beta_R/\gamma} - 1} = \frac{(\beta_R/\gamma)^{n-1}}{(n-1)!e^{\beta_R/\gamma}}.$$

Using this probability, the average fixation probability of a mutant in a single site is then given by

$$\rho^{\text{Single}} = \sum_{n=1}^{\infty}\mu^{\text{Init}}_n h_{\mathcal{M}}(\{(R, 1)^n, (M, 1)\}). \tag{15}$$

In this case, the hitting probability can be calculated by solving Eq. (7) when we limit the birth rate as follows

$$b(i, S) = \begin{cases} \beta_{U_i} & |S| < K,\\ 0 & |S| \geq K \end{cases} \tag{16}$$

where K is chosen to be large enough so that $\mathbb{P}(|S| \geq K) = 0$. This means that the maximum population size is K and the total number of states is $(K+1)^2$, because these are the total number of combinations of mutants and residents that sum to $\leq K$.

Fig. 2 shows the effect of competition rate on the fixation probability of a mutant in a single site (ρ^{Single}), which is calculated by solving for h using Eq. (7). To understand the behaviour here, we look at a comparable model with fixed population size. In models with fixed population size the population state is updated by choosing two individuals, one for birth and one for death. The offspring of the birth individual then replaces that of the death individual. Different update rules can be obtained by having natural selection act on birth or death. For death–Birth (dB) dynamics, an individual is randomly chosen for death and is then replaced by an offspring of an individual who is selected for birth proportional to their fitness (hence the uppercase in dB indicates selection). The fixation probability for dB EGT dynamics (Kaveh et al.,

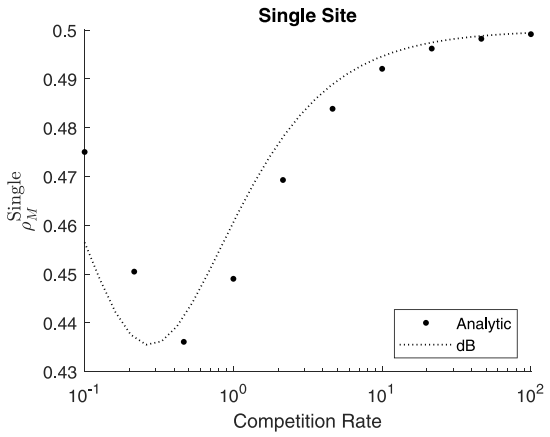

Fig. 2. Fixation probability of a mutant in a single site. Exact fixation probability is given by 'Analytic' plot, which is calculated using Eq. (15). Approximation using dB EGT dynamics is given by 'dB' plot, calculated using Eq. (18).

2015; Hindersin and Traulsen, 2015) is given by

$$\rho^{\text{dB}}(N,r) = \frac{N-1}{N}\frac{1-\frac{1}{r}}{1-\frac{1}{r^{N-1}}} = \frac{N-1}{N}\rho^{\text{Moran}}(N-1,r) \tag{17}$$

where N is the number of individuals, r is the relative fitness of a mutant to a resident and ρ^{Moran} is the Moran probability (Moran, 1959). As we will explain, we find that the dynamics in a single site for the birth–death-migration model resemble dB dynamics. By specifying a value for N and r, we can use ρ^{dB} to approximate ρ^{Single}. We set the relative fitness to $r = \beta_M/\beta_R$; this was selected because the different types differ in terms of their birth rate. To set N, we assume that with probability μ_n^{Init} a mutant arises in a population with n residents, so $N = n+1$. The maximum resident population size is set to K such that having a population size $\geq K$ tends to 0. Putting this together gives,

$$\rho_M^{\text{Single}} \approx \sum_{n=1}^{K} \mu_n^{\text{Init}} \rho^{\text{dB}}(n+1, \beta_M/\beta_R). \tag{18}$$

In Fig. 2 we see that, even though there is some discrepancy, similar behaviour is observed with both dB dynamics and the birth–death-migration model. The discrepancy between the two is due to fluctuating population size in the birth–death-migration model, which allows the population to be updated via a birth or death. With dB dynamics, the population size is fixed and can only be updated via a death–Birth event. Note that the discrepancy increases as the population size increases (competition rate decreases). Further insight can be obtained by looking at the components of ρ^{dB}. The component $(N-1)/N$ in ρ^{dB} is the probability that the initial mutant is not chosen to randomly die. This component dominates when the population size is small since the chance of the initial mutant randomly dying is higher. The component $\rho^{\text{Moran}}(N-1,r)$ captures the probability that the initial mutant fixates provided it does not randomly die. This component dominates as the population size gets larger since the probability of the initial mutant randomly dying decreases. This captures the behaviour observed for the single site case as follows. As the competition rate increases, the population size decreases and, therefore, the ability to survive this competition determines the fixation probability of a mutant. For a high competition rate the expected resident population size converges to 1, and ρ^{Single} converges to $\frac{1}{2}$ as both resident and mutant are equally likely to survive this intense competition. As the competition rate decreases, which increases the population size, the likelihood of surviving competition increases. The ability to reproduce therefore starts playing a more important role. The dip and recovery we see in ρ^{Single} observed in Fig. 2 is due to the birth rate of mutants we have chosen ($\beta_M = 2$). Changing the birth rate can alter this behaviour.

3.3. The low migration limit

We now return to the multiple site case and consider the low migration rate limit ($\lambda \to 0$). In this case, an initial mutant that appears on a site will die out or fixate before a migration event happens and therefore each site can be viewed as either a resident or mutant site prior to another migration event. The probability that a mutant fixates is then a two-step process. First, an initial mutant appears and fixates in a single site. Second, mutants then spread until they fixate in the population. The probability in the first step is given by ρ^{Single} for both low and high group tolerance. For low group tolerance we can obtain an analytic expression for the probability in the second step, but it is difficult for high group tolerance as we can have empty sites. We proceed by deriving an analytic expression for low group tolerance.

The rate $J_{x,y}^u$ at which a type u individual migrates from site x to y, is proportional to the expected number of individuals in site x who can migrate multiplied by the migration rate. In the case of low group tolerance (Eq. (11)), the rate $J_{x,y}^u$ is given by

$$J_{x,y}^u = \lambda W_{x,y} \sum_{n=2}^{\infty} n\pi_{n,x}^u = \lambda W_{x,y}\left(\frac{\beta_u/\gamma}{1-e^{-\beta_u/\gamma}} - \frac{\beta_u/\gamma}{e^{\beta_u/\gamma}-1}\right) = \lambda W_{x,y}\beta_u/\gamma. \tag{19}$$

Note that $\pi_{n,x}^u = \pi_n^u$ where the subscript for the site is included for clarity. To calculate the fixation probability of a type u immigrant arriving in site x, we need to account for the number of individuals currently present in site x. With probability $\pi_{n,x}^v$ there are n type v individuals present in site x and, therefore, the average fixation probability of a type u immigrant in site x is

$$\begin{aligned}\rho_{u,x}^{\text{Mig}} &= \sum_{n=1}^{\infty} \pi_{n,x}^v h_{\mathcal{F}(u)}(\{(v,x)^n,(u,x)\}) \\ &= \sum_{n=1}^{\infty} \frac{(\beta_v/\gamma)^n}{n!}\frac{1}{e^{\beta_v/\gamma}-1} h_{\mathcal{F}(u)}(\{(v,x)^n,(u,x)\})\end{aligned} \tag{20}$$

where $v \in \{M,R\}\setminus\{u\}$ and $\mathcal{F}$ gives the state that we fixate in, that is, $\mathcal{F}(M) = \mathcal{M}$ for mutant fixation, and $\mathcal{F}(R) = \mathcal{R}$ for resident fixation. Similar to obtaining the solution of ρ^{Single}, in ρ^{Mig} we can solve h using Eq. (7) by limiting the birth rate (Eq. (16)). Let $s \subseteq \{1,\ldots,N\} = \mathcal{X}$ represent a state of the population such that site x where $x \in s$ is a site occupied by mutants and a site y where $y \notin s$ represents a resident site. We can now define the probability that mutants fixate at the site level for low group tolerance and in the low migration limit as follows

$$\rho_s^{\text{Low Mig}} = \sum_{s' \subset \mathcal{X}} \frac{Q_{ss'}}{q_s}\rho_{s'}^{\text{Low Mig}} \tag{21}$$

with boundary conditions $\rho_{\emptyset}^{\text{Low Mig}} = 0$ and $\rho_{\mathcal{X}}^{\text{Low Mig}} = 1$, where $Q_{ss'}$ is the transition rate from state s to s', which is given by

$$Q_{ss'} = \begin{cases} \sum_{x\notin s} J_{x,y}^R \rho_{R,y}^{\text{Mig}} & \text{if } s' = s\setminus\{y\} \text{ for } y \in s, \\ \sum_{x\in s} J_{x,y}^M \rho_{M,y}^{\text{Mig}} & \text{if } s' = s\cup\{y\} \text{ for } y \notin s, \\ 0 & \text{otherwise,} \end{cases}$$

and q_s is the rate of transitioning away from state s, that is

$$q_s = \sum_{s' \subseteq \mathcal{X}} Q_{ss'}.$$

The average fixation probability of a mutant for low group tolerance and in the low migration limit is then given by

$$\rho^{\text{LGT}} = \sum_{x\in\mathcal{X}} p_x \rho_{M,x}^{\text{Single}} \rho_{\{x\}}^{\text{Low Mig}} \tag{22}$$

where $\rho_{M,x}^{\text{Single}} = \rho_M^{\text{Single}}$, but have included site index for clarity, and p_x is the probability a mutant appears in site x, which is proportional to

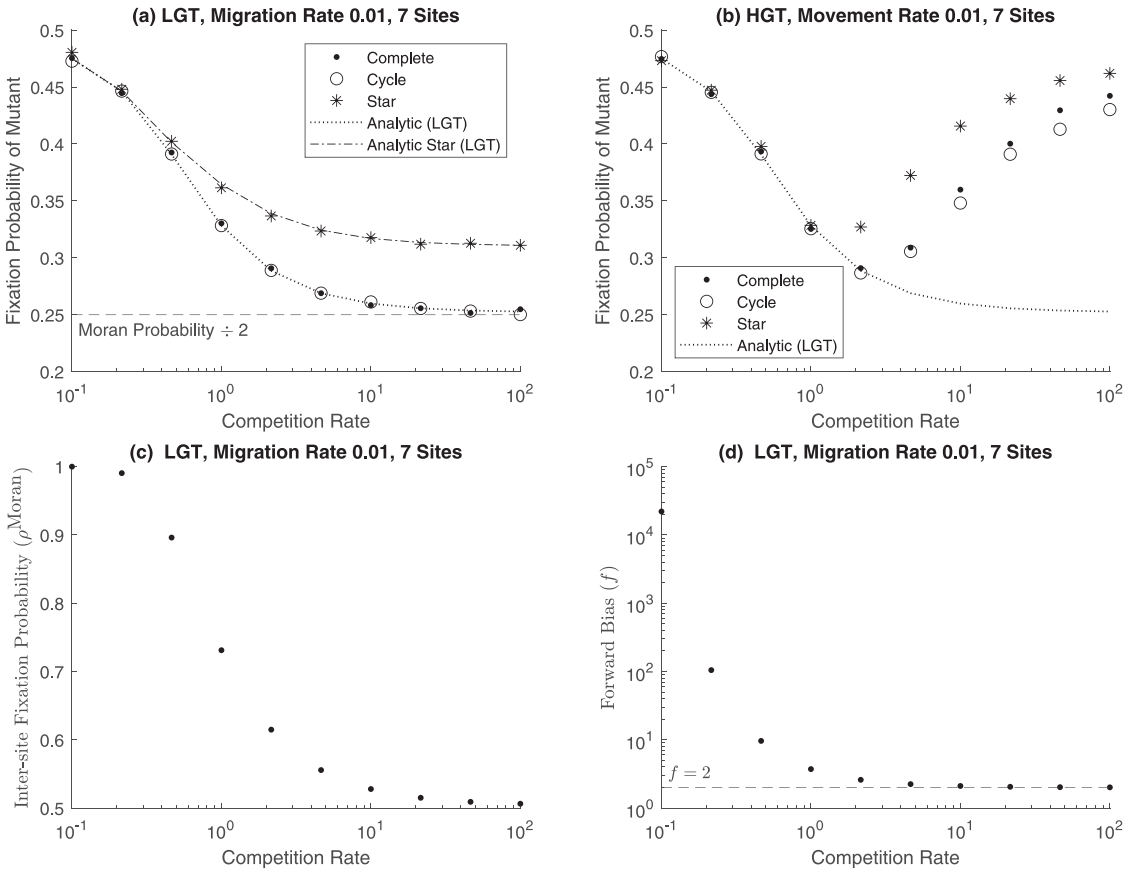

Fig. 3. Plots for the low migration case. (a) Fixation probability of a mutant for low group tolerance (LGT). (b) Fixation probability of a mutant for high group tolerance (HGT). In (a–b), 'Analytic (LGT)' is analytically calculated by Eq. (25). In (a), 'Anlaytic star (LGT)' is analytically calculated by solving Eq. (22) using the formula of Broom and Rychtář (2008). (c) Inter-site fixation probability of mutants in circulation networks for low group tolerance, that is, probability of fixating in entire population given that mutants have already fixated in one site. (d) The forward bias for mutants in circulation networks for the low group tolerance case.

the expected number of individuals on a site, that is,

$$p_x = \frac{\sum_{n=1}^{\infty} n\pi_{n,x}^R}{\sum_{y\in\mathcal{X}}\sum_{n=1}^{\infty} n\pi_{n,y}^R} = \frac{1}{N}.$$

Note that the intra-site dynamics are homogeneous, i.e. $\pi_{n,x}^R = \pi_{n,y}^R \ \forall x, y$, so the mutant appearance distribution is uniform. Since we have homogeneous intra-site dynamics, this simplifies the calculation of $\rho^{\text{Low Mig}}$ as now the network structure determines the complexity of the calculation. In particular, we can use the property where the sum of the incoming weights and the sum of the outgoing weights are the same to further simplify the calculation. In our case this would be the complete and cycle networks, and in general such networks are known as circulation networks (Lieberman et al., 2005). Circulation networks have constant forward bias for all transitory states (both residents and mutants exist). For a transitory state s the forward bias f is given by the rate of mutants increasing divided by the rate of residents decreasing; that is,

$$f = \frac{\sum_{x\in s} J_{x,y}^M \rho_{M,y}^{\text{Mig}}}{\sum_{x\notin s} J_{x,y}^R \rho_{R,y}^{\text{Mig}}}. \tag{23}$$

For constant forward bias, the closed form version of $\rho^{\text{Low Mig}}$ (Eq. (21)) is the Moran probability (Lieberman et al., 2005; Pattni et al., 2015), that is,

$$\rho^{\text{Moran}}(N, f) = \frac{1 - \frac{1}{f}}{1 - \frac{1}{f^N}}, \tag{24}$$

where N is the number of sites and f is the forward bias. Therefore, in the case of circulation networks, we can substitute $\rho_{\{x\}}^{\text{Low Mig}}$ with $\rho^{\text{Moran}}(N, f)$ for all x, so Eq. (22) simplifies to

$$\rho^{\text{LGT Circ}} = \rho_M^{\text{Single}} \rho^{\text{Moran}}(N, f). \tag{25}$$

For the star network, ρ^{LGT} (Eq. (22)) can be calculated using the formula in Broom and Rychtář (2008).

For low group tolerance, Fig. 3(a) shows that an increasing competition rate decreases the fixation probability for a low migration rate in all networks considered. We use the two components of $\rho^{\text{LGT Circ}}$ to understand why this is the case. The first component, ρ_M^{Single}, describes the intra-site dynamics, which we have already explained. The second component, ρ^{Moran}, describes the inter-site dynamics, or how mutants spread once they have fixated on a single site. The inter-site dynamics are shown in Fig. 3(c), where we see that ρ^{Moran} is a sigmoid shaped curve whose shape is explained by the forward bias (f) that is shown in Fig. 3(d). For a decreasing competition rate we see that

$$\lim_{\gamma\to 0} f \approx \infty \Rightarrow \rho^{\text{Moran}} \to 1 \Rightarrow \lim_{\gamma\to 0} \rho^{\text{LGT Circ}} \approx \lim_{\gamma\to 0} \rho^{\text{Single}}. \tag{26}$$

This means that for a low competition rate a mutant fixating on one site is sufficient to guarantee that it goes on to fixate in the entire population. For an increasing competition rate we see that

$$\lim_{\gamma\to\infty} f \approx \lim_{\gamma\to\infty} \frac{\frac{(\beta_M/\gamma)^2}{2!}\frac{1}{\exp(\beta_M/\gamma)-1}\frac{(\beta_R/\gamma)^1}{1!}\frac{1}{\exp(\beta_R/\gamma)-1}\frac{1}{2}}{\frac{(\beta_R/\gamma)^2}{2!}\frac{1}{\exp(\beta_R/\gamma)-1}\frac{(\beta_M/\gamma)^1}{1!}\frac{1}{\exp(\beta_M/\gamma)-1}\frac{1}{2}} = \frac{\beta_M}{\beta_R} \Rightarrow$$

$$\lim_{\gamma\to\infty} \rho^{\text{LGT Circ}} \approx \frac{1}{2}\rho^{\text{Moran}}(N, \beta_M/\beta_R) \tag{27}$$

where when calculating f we have assumed that there are two individuals when a migration event happens and that an immigrant arrives to a site with one individual only so fixates with probability $\frac{1}{2}$. Note that

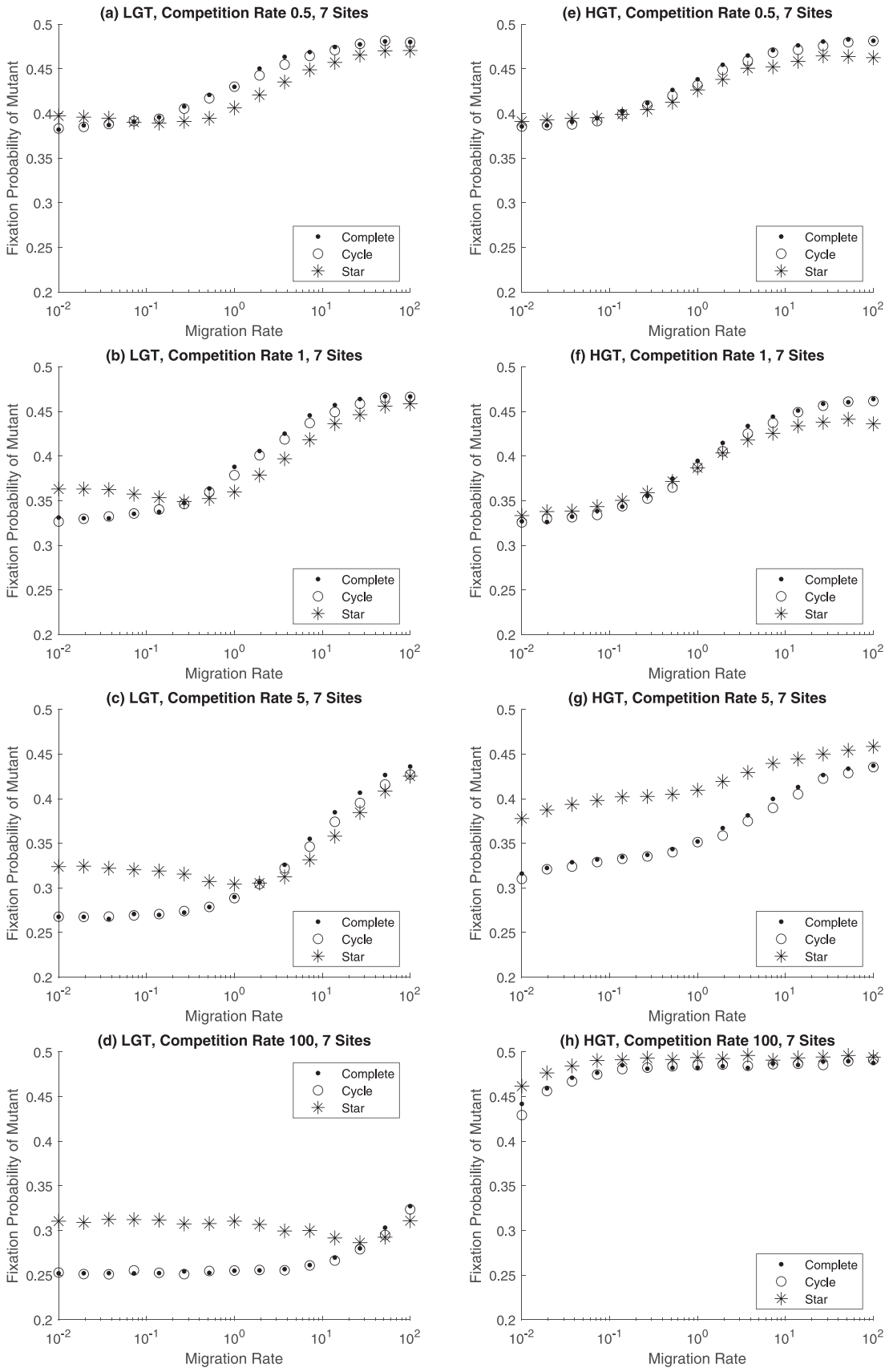

Fig. 4. Fixation probability of a mutant plotted against the migration rate of individuals for different competition rates. Each network has 7 sites and birth rate of mutants is 2. Figures (a–d) there is low group tolerance (LGT). Figures (e–g) there is high group tolerance (HGT).

in this case the forward bias converges to the relative birth rates of the individuals ($\beta_M/\beta_R = 2$), which means that each site can be viewed as a single individual as in the case of EGT.

In the star network for low group tolerance Fig. 3(a) shows that it follows a similar pattern to the complete and cycle networks. However, the fixation probability in the star network is higher for high competition rates but converges as the competition rate decreases. Since $\lambda \to 0$, mutants are likely to appear on leaf sites in a star network as the combined number of individuals on leaf sites is higher than the centre site. Appearing on leaf sites is beneficial because the way in which W is defined for the star network (Eq. (13)) allows leaf sites to act as source sites, i.e. are net exporters of individuals. This is because the outgoing weight from a leaf site to the centre is 1 whereas the outgoing weight from the centre site to a leaf site is $1/(N-1)$, and therefore individuals are more likely to migrate from a leaf site to the centre site than vice versa. For low competition rate, convergence occurs since the intra-site dynamics are identical for all networks and, as explained earlier, if a mutant fixates on one site, it is essentially guaranteed to fixate in the entire population. On the other hand, as the competition rate increases, which gives residents a better chance to prevent invasion, the divergence in the fixation probability between the star and circulation networks becomes more apparent.

For high group tolerance, Fig. 3(b) shows a similar pattern to low group tolerance where fixation probability decreases as the competition rate increases. High group tolerance allows empty sites, however, when competition rate is low, the likelihood of empty sites decreases and the intra-site dynamics would be similar to that of low group tolerance. The fixation probabilities are therefore identical to the low group tolerance case for low competition rate. As the competition rate increases, the chance of having empty sites increases, changing the behaviour observed. In particular, the population starts converging to a population size of 1 as individuals start dying off when they meet. This means that as the competition rate increases the fixation probability starts converging to $\frac{1}{2}$ as the likelihood that a mutant appears in a population with one resident increases. Overall, the fixation probability starts decreasing then increasing again as the competition rate increases.

3.4. General migration rate

In this section we consider the case for a general migration rate ($\lambda > 0$). The fixation probability in this case is calculated via simulation.

3.4.1. Effect of increasing migration rate

Migration allows individuals to escape competition as shown in Fig. 4 where the fixation probability increases with the migration rate. The way in which this plays out depends upon the competition rate, network structure and group tolerance. The effects of these are explained in the following.

For low group tolerance, Fig. 4 (a–d) shows that as the migration rate increases the fixation probability starts increasing and plateaus earlier for low competition than high competition. However, as $\lambda \to \infty$ there would be a larger overall increase in the fixation probability for high competition. In the initial growth and plateau phases of the fixation probability, the complete and cycle networks follow each other closely and are indistinguishable. As the growth in the fixation probability accelerates, there is higher acceleration in the complete network than the cycle network. The key factor here is local correlation between groups on neighbouring sites on the cycle. For low migration rates fixation probabilities are low and similar for both cycle and complete networks. New individuals are likely to be born into bigger groups, as there are more potential parents, but cannot move on, so face increased competition. As they hardly move, network does not matter. For intermediate migration rates fixation probabilities are intermediate, but differ for the two types. New individuals are born to bigger groups, but there is some dispersal so they face an intermediate level of competition. Here dispersal happens to some extent, and so the network does matter. For high migration rates fixation probabilities are high and similar for the two types. New individuals are born in bigger groups but then there is rapid dispersal so they live in 'average' groups. As migration is so far they mix well, so network does not matter. To illustrate this point further, Fig. 5 shows the fixation probability in the case of a neutral mutant, i.e. $\beta_R = \beta_M = 1$. If there is no correlation between the sites, the fixation probability would be identical for the complete and cycle networks. There is correlation as we see a difference in the fixation probabilities, which happens for intermediate migration rates. For the star network, as λ increases we see that there is an initial dip in the fixation probability before it starts increasing. This is because increasing the migration rate results in the number of individuals in the centre site becoming larger than a leaf site. This increases the likelihood of a mutant appearing in the centre site which is a sink, i.e. a net importer of individuals as individuals are more likely to die than reproduce, which adversely affects the fixation probability. This dip happens earlier for a lower competition rate and, after this dip, the fixation probability remains below that of the complete and cycle networks.

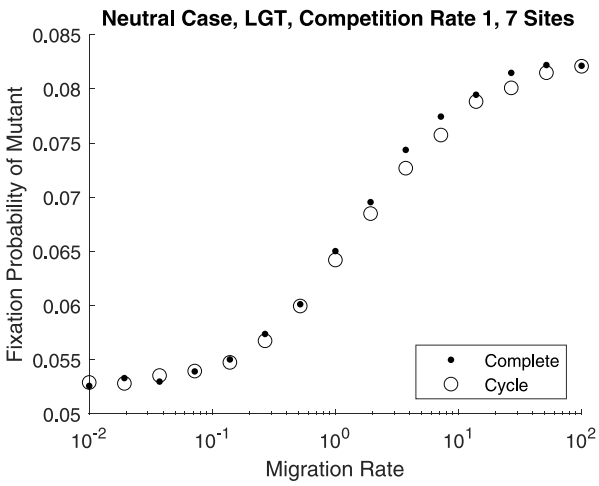

Fig. 5. Fixation probability in the neutral case ($\beta_R = \beta_M = 1$). This plot was generated using 10^6 simulations.

For high group tolerance Fig. 4 (e–h) shows that the behaviour observed is similar to low group tolerance when competition rate is low but vastly different for a higher competition rate. For low competition rate, the intra-site dynamics are similar in high and low group tolerance. In particular, for a low competition rate the likelihood of there being empty sites is low even as the migration rate increases. On the other hand, for a high competition rate the likelihood of empty sites increases. This means that a mutant arises in a population with fewer individuals than in the low group tolerance case. This is observed in Fig. 4(g) and (h). In (g), the star network has a higher fixation probability for all migration rates than the complete and cycle networks. This is because individuals are more likely to meet in the centre site resulting in death due to competition, which drives the population size down. This effect is substantial for a high competition rate as seen in (h). As the migration rate increases, the fixation probability in all networks swiftly converges to $\frac{1}{2}$ since the population size is converging to 1.

Fig. 6 shows the effect of migration rate as the number of sites increases. Fig. 6(a) considers the low migration limit for low group tolerance in circulation networks. We see that for a low competition rate ($\gamma = 0.1$), the fixation probability remains the same as the number of sites increases. This was previously explained using Eq. (26), where fixating in one site was sufficient to guarantee fixation in all sites. This effect carries over for higher competition rates, but the number of sites required to guarantee fixation increases. We observe that the

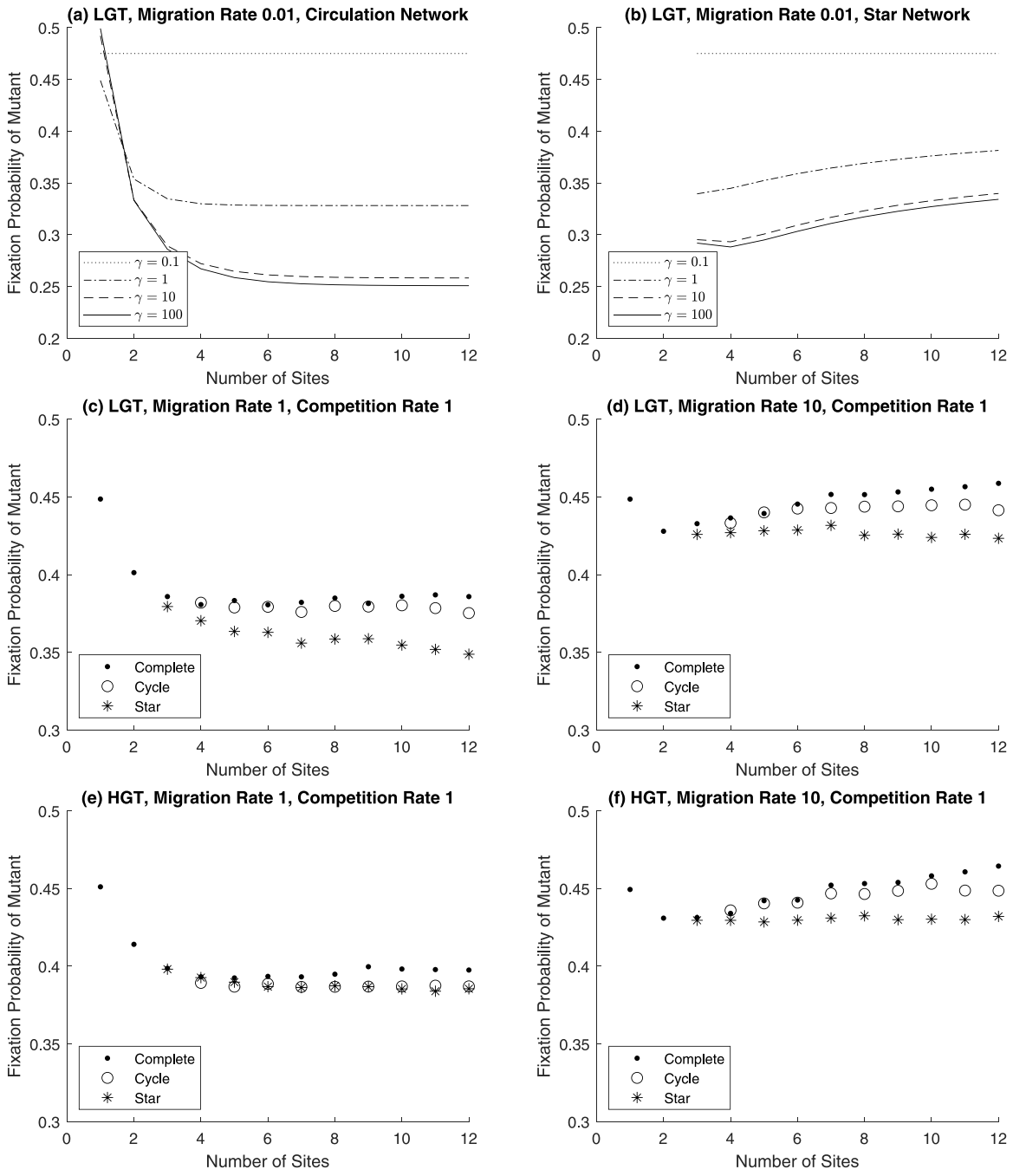

Fig. 6. Effect of increasing the number of sites on the fixation probability. Figures (a–d) are for low group tolerance (LGT) and figures (e–f) are for high group tolerance (HGT). Figure (a) is analytically calculated using Eq. (25) for Circulation networks, and figure (b) is calculated using the analytical formula for the star network. Figures (c–f) are generated using 10^5 simulations. For the cycle network, the plot starts from 4 sites as fewer than 4 sites classifies as a complete network. For the star network, the plot starts from 3 sites as this is the minimum number of sites required to construct a star network.

fixation probability initially starts to decrease as the number of sites increases, but once we reach the point where the number of sites guarantees fixation, the fixation probability will flatline. For example, we see that for a high competition rate ($\gamma = 100$) the fixation probability flatlines after approximately 7 sites, that is, fixating in 7 sites guarantees fixation in the entire population. This effect is also evident in circulation networks for low group tolerance and high group tolerance with a relatively low migration rate of 1 as seen in Figs. 6 (c) and (e). However, when the migration rate is increased ($\lambda = 10$), for both low and high group tolerance there is a slight dip as the number of sites increases, but recovers to the one site level as seen in Figs. 6 (d) and (f). This is because the population effectively behaves as one big unit when the migration rate is high, with this being more pronounced with a higher number of sites as there are more individuals. In the star network (Fig. 6(b)), for low competition the effect of increasing the number of sites is the same as for circulation networks i.e. fixating in one site guarantees fixation in the entire population. For a higher competition rate, the fixation probability increases with the number of

sites. This is because we are adding a leaf site each time the number of sites increases, which increases the likelihood of a mutant appearing on a leaf site. As explained earlier, leaf sites are source sites and therefore beneficial for a mutant. As the migration rate increases to 1, the fixation probability decreases in the star network with an increasing number of sites for low group tolerance (Fig. 6(c)). This is because the higher migration rate results in an increased number of individuals in the centre site, which increases the likelihood of the initial mutant appearing in the centre site. As the centre site is a sink, it is less beneficial for mutants. This does not happen for high group tolerance (Fig. 6(e)), as most leaf sites are likely to remain empty with most of the population being present in the centre site. The population therefore behaves as one large unit clustered in the centre site. As the migration is increased to 10, for both low and high group tolerance (Fig. 6(d) and (f)), the fixation probability in the star network remains constant as the number of sites is increased. This is because individuals are mixing with each other much more, nullifying the effect of network structure in both cases.

3.4.2. Comparison to low migration limit

For low group tolerance Fig. 7 (a–c) shows that there is initially similar behaviour to the low migration limit, but gradually breaks down as the migration rate keeps increasing. The fixation probability in the complete and cycle networks are higher than in the low migration limit as migration enables escaping competition. This difference is less apparent for high competition as it requires a much larger migration rate to make a significant difference. In the low migration limit, the star network has a higher fixation probability than the complete and cycle networks, and converges as the competition rate decreases. Here, the star network initially has a lower fixation probability for a low competition rate. As the competition rate increases this difference gradually diminishes and eventually the fixation probability surpasses that of the complete and cycle networks. This behaviour is explained by the decreasing likelihood of a mutant appearing in the centre site. When the competition rate is low, there are more individuals in the centre site than there are on a leaf site, thus there is an increased likelihood of a mutant appearing on the centre site. However, this likelihood starts decreasing as the competition rate increases, which reduces the number of individuals in the centre site. Since the centre site acts as a sink, i.e. it is a net importer of individuals, it suppresses the fixation probability.

For high group tolerance Fig. 7 (d–f) shows that the fixation probability decreases then increases as the competition rate increases. This behaviour is significantly different to that observed in the low migration limit. For low competition rate ($\gamma \leq 1$) the behaviour is similar to that of low group tolerance (Fig. 7 (a–c)), this means that the intra-site dynamics are similar for both cases. That is, even though high group tolerance allows for empty sites in their intra-site dynamics, this is unlikely when the competition rate is lower. As the competition increases ($\gamma > 1$), empty sites are more likely as a death is more likely to occur whenever moving individuals come into contact with one another. This drives the population size down. We observe that as the competition rate increases, the fixation probability turns and starts to increase, eventually converging to 0.5. This implies that the entire resident population prior to a mutant arising is converging to 1. When comparing between networks, the fixation probability in the star network turns first and converges faster to 0.5. This is because individuals are more likely to meet in the centre site in a star network which drives the population size down faster than the complete and star networks.

4. Discussion

In this paper we have proposed an evolutionary framework where the population is updated through individual birth, death and migration. This is based on the individual-based framework of Champagnat et al. (2006) which we have adapted to allow migration between a network of sites. An alternative to a network of sites is to consider continuous spatial structure (Champagnat and Méléard, 2007). The approach we have used here based on discrete space allows us to understand the effect of migration on an evolutionary process for different network topologies, which have been shown to amplify the effect of selection in the evolutionary graph theory (EGT) framework (Lieberman et al., 2005; Broom and Rychtář, 2008; Shakarian et al., 2012; Hindersin and Traulsen, 2015; Yagoobi and Traulsen, 2021). In EGT population size and distribution is fixed, which is achieved by coupling migration with birth and death. Here, migration is a separate process and not coupled with birth or death therefore allowing for demographic fluctuations (e.g. changes in population size and distribution) that are shown to affect trait fixation (Czuppon and Gokhale, 2018). The framework allows for overlapping evolutionary and ecological timescales but in this paper we focus on the rare mutation limit. This means the population evolves in adaptive sweeps (Gerrish and Lenski, 1998) where a mutant either fixates or goes extinct prior to another mutant arising. This allows the effect of network structure on evolution to be measured in terms of the fixation probability of a mutant. Considering a simplistic model initially allows us to identify and understand the parameters that are of interest. We can then consider more biologically relevant models with continuous mutations where alternative measures of mutant success are required such as the mutation-selection equilibrium (Yagoobi et al., 2018; Sharma and Traulsen, 2022).

To control the migration of individuals we have provided an extreme example of a positive density-dependent migration regime where individuals move only when they are in a group. In general, non-linear effects can be assumed due to there being varying effects at different densities (Bowler and Benton, 2005). We can also have negative density-dependent migration where individuals migrate when the number of individuals on a site falls, which can be explained by increased predation (Kuussaari et al., 1996). Migration plays a significant role when complex strategies are involved such as in the evolution of cooperation (Ichinose et al., 2013; Erovenko et al., 2019). In our case, individuals only differed in terms of their birth rate, so we employed a simplistic migration regime where individuals move only when in a group or move regardless of group composition. This in turn enabled us to obtain analytical results in the low migration limit and allows us to make comparisons with models with fixed population size where all sites are always occupied (Lieberman et al., 2005; Yagoobi and Traulsen, 2021).

By considering a model with variable population size and distribution we can capture effects that are not present in models with fixed size and distribution. In particular, variable population size and distribution affects the mutant appearance distribution which impacts the fixation probability. To enable comparisons with models with fixed and finite population size, we need to obtain a comparable mutant appearance distribution. Models with fixed size and distribution can use a uniform distribution or an alternative such as the temperature-weighted mutant appearance distribution (Allen and Tarnita, 2014). In a uniform distribution, a mutant is equally likely to take the place of a resident. In a temperature-weighted distribution, a mutant takes the place of a resident proportional to their temperature, which is their likelihood of being replaced. One way to artificially apply either of these schemes in populations with variable size and distribution is to fix the initial state and then replace one resident with a mutant using the uniform or temperature weighted distribution. This approach is sufficient for specific purposes, for example, understanding how EGT dynamics can be derived from a model with eco-evolutionary dynamics (Pattni et al., 2021). The approach used here, considers all the states of the system prior to a mutation arising and have therefore had to resort to other options to obtain a mutant appearance distribution that is close to models with fixed size and distribution. To obtain a distribution that is akin to the EGT framework (Lieberman et al., 2005) where each site is occupied by one individual, we assumed a high competition

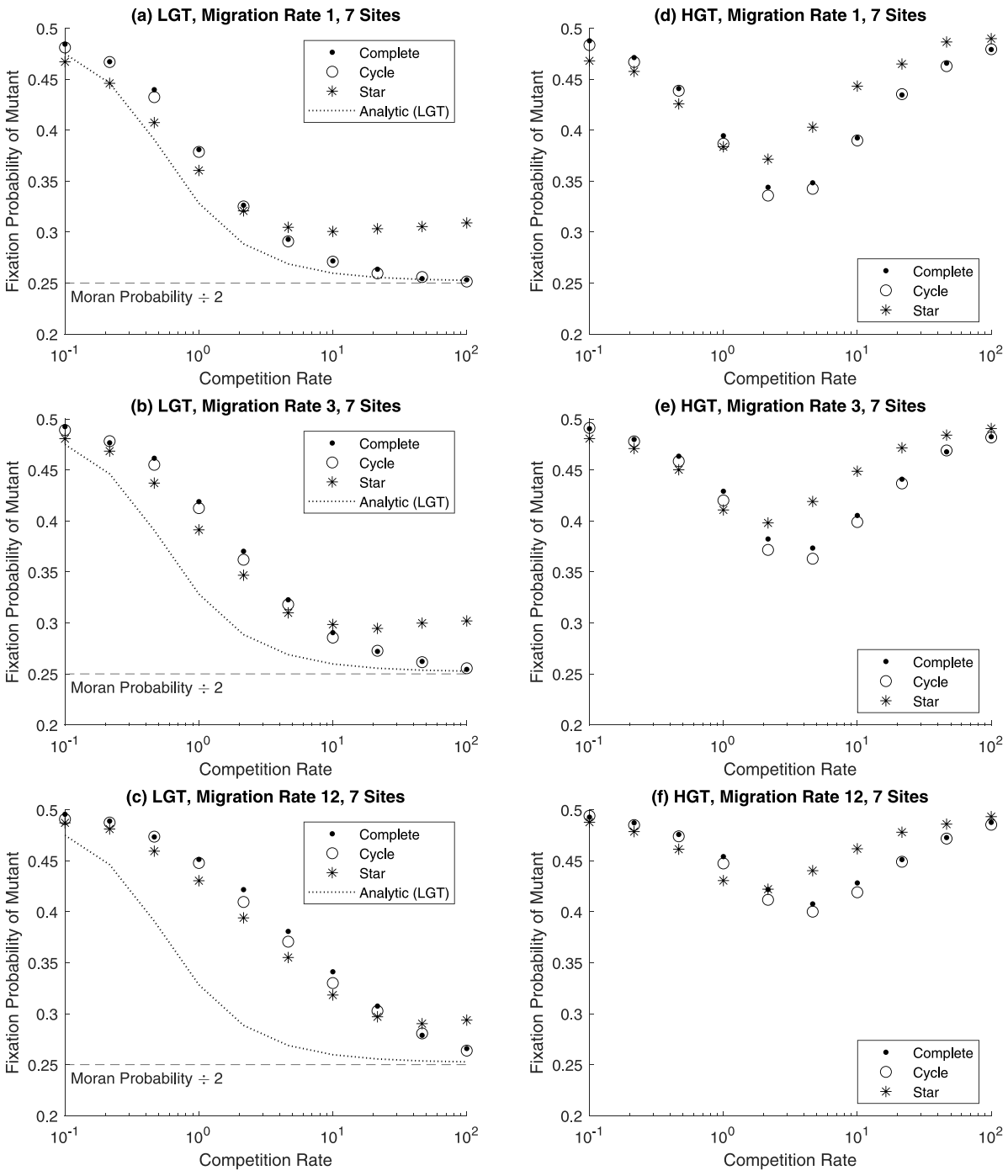

Fig. 7. Fixation probability in the cycle, complete and star networks plotted against the competition rate γ for different migration rates. Figures (a–c) have low group tolerance (LGT). 'Analytic (LGT)' plot is calculated using Eq. (25), which represents the low migration limit. Figures (e–f) have high group tolerance (HGT).

rate so that competition would kill off all but one individual in a site and assumed that individuals have low tolerance so only move when they are in a group resulting in all sites being occupied. Even then the mutant appearance distribution is slightly different as EGT does not take into account the competition faced by a mutant to take over a site. The mutation dynamics (the process of a mutant appearing in the population) are simpler in EGT as a mutant simply replaces a resident and does not compete for that site as it will break the fixed population size assumption (in a population size of n, the population size has to temporarily be $n+1$ to account for the appearance of a mutant). The effect of this is that the fixation probability with mutation dynamics in our model is weighted by the probability of an initial mutant competing for a space within the population. Whilst this is a feature of our model, this can be considered in EGT when defining the mutant appearance distribution.

In models with fixed population size and distribution a network's effect is dependent upon the mutant appearance distribution used (Tkadlec et al., 2019; Allen et al., 2021; Yagoobi and Traulsen, 2021). In particular, the mutation appearance distribution chosen can increase or decrease the chances of a mutant appearing on beneficial sites. In the birth–death-migration model considered here, the mutant appearance distribution changes with the migration rate. Having the mutant appearance distribution change within the model allows investigation of a wider range of behaviours such as the optimal mutation strategy for

bacteria that take into account migration and spatial structure (Denamur and Matic, 2006). This is because the effect of networks in terms of amplifiers or suppressors becomes more fluid as they can switch between the two. We observed that the star network switches from an amplifier to suppressor as the migration rate increases. We also uncovered subtle differences between networks with shared properties. Networks where every site has a balanced inflow and outflow of individuals are shown to have identical fixation probability (Maruyama, 1970, 1974; Lieberman et al., 2005; Yagoobi and Traulsen, 2021). In our case, the complete and cycle networks that satisfy this property were shown to have subtle differences for intermediate migration rates but were otherwise similar in behaviour. Such subtleties can play a key role in neutral mutations, for example, low network connectivity can increase a population's susceptibility to neutral virus strains (Marquioni and De Aguiar, 2021).

In summary, we have presented a network-structured population evolution framework where birth, death and migration are uncoupled. We study the effect of network structure in the rare mutation limit and have shown how the mutant appearance distribution affects the success of an invading mutant. Future work will move away the rare mutation limit so that overlapping evolutionary and ecological timescales can be considered in the context of network structure.

CRediT authorship contribution statement

Karan Pattni: Writing – original draft, Writing – review & editing, Formal analysis. **Wajid Ali:** Writing – original draft, Writing – review & editing, Formal analysis. **Mark Broom:** Conceptualization, Writing – review & editing, Supervision, Methodology. **Kieran J. Sharkey:** Conceptualization, Writing – review & editing, Supervision, Methodology.

Declaration of competing interest

There are no conflicts of interest to declare.

Acknowledgements

KP and KS acknowledge funding from EPSRC, United Kingdom project grant EP/T031727/1. This project has received funding from the European Union's Horizon 2020 research and innovation programme under grant agreement No 955708.

Appendix. Simulation details

The evolutionary process is simulated using the Gillespie algorithm (Gillespie, 1976, 1977). Recall that the infinitesimal generator (Eq. (1)) describing the evolutionary process is as follows

$$\begin{aligned}\mathcal{L}\phi(S) = &\sum_{i\in S}[1-\mu(i)]b(i,S)[\phi(S\cup\{i\})-\phi(S)]\\ &+\sum_{i\in S}\mu(i)b(i,S)\int_{\mathbb{R}^l}[\phi(S\cup\{(u,X_i)\})-\phi(S)]M(U_i,u)du\\ &+\sum_{i\in S}d(i,S)[\phi(S\backslash\{i\})-\phi(S)]\\ &+\sum_{i\in S}\sum_{x\in\mathcal{X}}m(i,x,S)[\phi(S\cup\{(U_i,x)\}\backslash\{i\})-\phi(S)].\end{aligned}$$

For this process, let $T(k)$ and $S(k)$ respectively be the time and state after k events. The simulation follows the following steps:

1. The time, $T(k+1)$, when the next event happens is given by

   $$T(k+1) = T(k) - \frac{\ln(\text{Unif}(0,1))}{\lambda_k}$$

   where $\text{Unif}(0,1)$ is uniformly distributed random number in the range $(0,1)$ and

   $$\lambda_k = \sum_{i\in S(k)}\sum_{x\in\mathcal{X}} b(i,S(k)) + d(i,S(k)) + m(i,x,S(k)).$$

2. The next state, $S(k+1)$, is determined by:

   - Birth without mutation: The probability that I_i gives birth to an offspring with the same type is

     $$[1-\mu(i)]\frac{b(i,S(k))}{\lambda_k}$$

     then $S(k+1) = S(k)\cup\{(U_i,X_i)\}$.
   - Birth with mutation: The probability that I_i gives birth to an offspring with type w is

     $$\mu(i)M(U_i,w)\frac{b(i,S(k))}{\lambda_k}.$$

     then $S(k+1) = S(k)\cup\{(w,X_i)\}$.
   - Death: The probability that I_i dies is

     $$\frac{d(i,S(k))}{\lambda_k}$$

     then $S(k+1) = S(k)\setminus\{i\}$.
   - Migration: The probability that I_i migrates to site n is

     $$\frac{m(i,n,S(k))}{\lambda_k}$$

     then $S(k+1) = S(k)\cup\{(U_i,n)\}\setminus\{i\}$.

3. Repeat steps 1 and 2 as required.

For the birth–death-migration model to simulate the hitting probability (Eq. (7)),

$$\mathcal{L}h_{\mathcal{M}}(S) = 0$$

with boundary conditions $h_{\mathcal{M}}(S) = 1$ for $S\in\mathcal{M}$ and $h_{\mathcal{M}}(S) = 0$ for $S\in\mathcal{R}$, we first need to determine the initial state in the rare mutation limit. To do this, we set $T(0) = 0$, $\mu(i) = 1^{-4}\ \forall i$, $M(R,M) = 1$ and choose $S(0)\in\mathcal{R}$ such that $S(0)$ is at the carrying capacity in the deterministic system. This is an added step taken to ensure that the stochastic system is fluctuating around its carrying capacity prior to a mutant arising. The deterministic system is obtained by assuming that, rather than there being a discrete number of individuals, the number of individuals is continuous. Let $e_1(t),\dots,e_N(t)$ be the number of residents at time t in each site. For low group tolerance (Eq. (11)), we want the solution to the system (dropping t for brevity)

$$\frac{de_x}{dt} = \beta_R e_x - \gamma e_x(e_x-1) + \sum_y \lambda(e_y-1)W_{y,x} - \lambda(e_x-1)W_{x,y} = 0, \tag{28}$$

where the first term accounts for birth, second term death, third term is immigration and fourth term is emigration. Note that migration takes place only if the number of individuals on a site is >1. Similarly, for high group tolerance (Eq. (12)) we want the solution to

$$\frac{de_x}{dt} = \beta_R e_x - \gamma e_x(e_x-1) + \sum_y \lambda e_y W_{y,x} - \lambda e_x W_{x,y} = 0, \tag{29}$$

the terms are as in the low group tolerance case but migration in this case happens when the individuals on a site is >0. After obtaining $e_1(t),\dots,e_N(t)$, we round up to the nearest integer and set $S(0)$ to this. We then repeat steps 1 and 2 as outlined above until a mutant appears. Once a mutant appears, we use this as the initial state to calculate the hitting probability. To continue the simulation, we set $\mu(i) = 0\ \forall i$ and continue the simulation until we hit a state in $\mathcal{R}$ or $\mathcal{M}$. This is one run of the simulation which we repeat to generate multiple simulations. Note that initialising the population in this way takes into account the mutant appearance distribution ($p_{x,S}$) since a mutant is more likely to appear in a site with more individuals. The average fixation probability of a mutant is then given by $N_{\text{mut}}/N_{\text{sim}}$ where N_{sim} and N_{mut} are the total number of simulations and the number of simulations that hit $\mathcal{M}$ respectively.

References

Allen, B., Sample, C., Steinhagen, P., Shapiro, J., King, M., Hedspeth, T., Goncalves, M., 2021. Fixation probabilities in graph-structured populations under weak selection. In: Traulsen, A. (Ed.), PLoS Comput. Biol. 17 (2), e1008695. http://dx.doi.org/10.1371/journal.pcbi.1008695.

Allen, B., Tarnita, C.E., 2014. Measures of success in a class of evolutionary models with fixed population size and structure. J. Math. Biol. 68 (1–2), 109–143.

Bauer, S., Klaassen, M., 2013. Mechanistic models of animal migration behaviour–their diversity, structure and use. J. Anim. Ecol. 82 (3), 498–508.

Bowler, D.E., Benton, T.G., 2005. Causes and consequences of animal dispersal strategies: Relating individual behaviour to spatial dynamics. Biol. Rev. 80 (2), 205–225.

Broom, M., Pattni, K., Rychtář, J., 2019. Generalized social dilemmas: The evolution of cooperation in populations with variable group size. Bull. Math. Biol. 81, 4643–4674.

Broom, M., Rychtář, J., 2008. An analysis of the fixation probability of a mutant on special classes of non-directed graphs. Proc. R. Soc. Lond. Ser. A Math. Phys. Eng. Sci. 464 (2098), 2609–2627.

Broom, M., Rychtář, J., 2012. A general framework for analysing multiplayer games in networks using territorial interactions as a case study. J. Theoret. Biol. 302, 70–80.

Champagnat, N., Ferrière, R., Méléard, S., 2006. Unifying evolutionary dynamics: From individual stochastic processes to macroscopic models. Theor. Popul. Biol. 69 (3), 297–321. http://dx.doi.org/10.1016/j.tpb.2005.10.004.

Champagnat, N., Méléard, S., 2007. Invasion and adaptive evolution for individual-based spatially structured populations. J. Math. Biol. 55 (2), 147–188. http://dx.doi.org/10.1007/s00285-007-0072-z.

Czuppon, P., Gokhale, C.S., 2018. Disentangling eco-evolutionary effects on trait fixation. Theor. Popul. Biol. 124, 93–107. http://dx.doi.org/10.1016/j.tpb.2018.10.002.

Denamur, E., Matic, I., 2006. Evolution of mutation rates in bacteria. Mol. Microbiol. 60 (4), 820–827.

Erovenko, I.V., Bauer, J., Broom, M., Pattni, K., Rychtář, J., 2019. The effect of network topology on optimal exploration strategies and the evolution of cooperation in a mobile population. Proc. R. Soc. Lond. Ser. A Math. Phys. Eng. Sci. 475 (2230), 20190399.

Fletcher, J.A., Doebeli, M., 2009. A simple and general explanation for the evolution of altruism. Proc. R. Soc. Lond. Ser. B: Biol. Sci. 276 (1654), 13–19.

Fournier, N., Méléard, S., 2004. A microscopic probabilistic description of a locally regulated population and macroscopic approximations. Ann. Appl. Probab. 14 (4), 1880–1919. http://dx.doi.org/10.1214/105051604000000882.

Frean, M., Rainey, P.B., Traulsen, A., 2013. The effect of population structure on the rate of evolution. Proc. R. Soc. Lond. Ser. B: Biol. Sci. 280 (1762), 20130211.

Gerrish, P.J., Lenski, R.E., 1998. The fate of competing beneficial mutations in an asexual population. Genetica 102, 127–144.

Gillespie, D.T., 1976. A general method for numerically simulating the stochastic time evolution of coupled chemical reactions. J. Comput. Phys. 22 (4), 403–434.

Gillespie, D.T., 1977. Exact stochastic simulation of coupled chemical reactions. J. Phys. Chem. 81 (25), 2340–2361.

Grenfell, B.T., Pybus, O.G., Gog, J.R., Wood, J.L., Daly, J.M., Mumford, J.A., Holmes, E.C., 2004. Unifying the epidemiological and evolutionary dynamics of pathogens. Science 303 (5656), 327–332.

Hadjichrysanthou, C., Broom, M., Rychtář, J., 2011. Evolutionary games on star graphs under various updating rules. Dynam. Games Appl. 1 (3), 386.

Hanski, I., 1998. Metapopulation dynamics. Nature 396, 41.

Hindersin, L., Traulsen, A., 2014. Counterintuitive properties of the fixation time in network-structured populations. J. R. Soc. Interface 11 (99), 20140606. http://dx.doi.org/10.1098/rsif.2014.0606.

Hindersin, L., Traulsen, A., 2015. Most undirected random graphs are amplifiers of selection for birth-death dynamics, but suppressors of selection for death-birth dynamics. PLoS Comput. Biol. 11 (11), e1004437.

Ichinose, G., Saito, M., Sayama, H., Wilson, D.S., 2013. Adaptive long-range migration promotes cooperation under tempting conditions. Sci. Rep. 3 (1), 2509.

Kaveh, K., Komarova, N.L., Kohandel, M., 2015. The duality of spatial death–birth and birth–death processes and limitations of the isothermal theorem. Roy. Soc. Open Sci. 2 (4), 140465.

Kimura, M., Weiss, G.H., 1964. The stepping stone model of population structure and the decrease of genetic correlation with distance. Genetics 49 (4), 561.

Kölzsch, A., Kleyheeg, E., Kruckenberg, H., Kaatz, M., Blasius, B., 2018. A periodic Markov model to formalize animal migration on a network. Roy. Soc. Open Sci. 5 (6), 180438.

Kuussaari, M., Nieminen, M., Hanski, I., 1996. An experimental study of migration in the Glanville fritillary butterfly Melitaea cinxia. J. Animal Ecol. 791–801.

Lieberman, E., Hauert, C., Nowak, M., 2005. Evolutionary dynamics on graphs. Nature 433 (7023), 312–316.

Liu, Q.-X., Rietkerk, M., Herman, P.M., Piersma, T., Fryxell, J.M., van de Koppel, J., 2016. Phase separation driven by density-dependent movement: A novel mechanism for ecological patterns. Phys. Life Rev. 19, 107–121.

Marquioni, V.M., De Aguiar, M.A.M., 2021. Modeling neutral viral mutations in the spread of SARS-CoV-2 epidemics. In: Sendiña-Nadal, I. (Ed.), PLOS ONE 16 (7), e0255438. http://dx.doi.org/10.1371/journal.pone.0255438.

Maruyama, T., 1970. On the probability of fixation of mutatnt genes in subdivided populations. Genet. Res. 15, 221–225.

Maruyama, T., 1974. A simple proof that certain quantities are independent of the geographical structure of population. Theor. Popul. Biol. 5 (2), 148–154.

Moran, P.A.P., 1959. The survival of a mutant gene under selection. J. Aust. Math. Soc. 1 (01), 121. http://dx.doi.org/10.1017/S1446788700025155.

Pattni, K., Broom, M., Rychtář, J., Silvers, L.J., 2015. Evolutionary graph theory revisited: When is an evolutionary process equivalent to the Moran process? Proc. R. Soc. Lond. Ser. A Math. Phys. Eng. Sci. 471 (2182), 20150334.

Pattni, K., Overton, C.E., Sharkey, K.J., 2021. Evolutionary graph theory derived from eco-evolutionary dynamics. J. Theoret. Biol. 519, 110648. http://dx.doi.org/10.1016/j.jtbi.2021.110648.

Rosenquist, J.N., 2010. The spread of alcohol consumption behavior in a large social network. Annal. Internal Med. 152 (7), 426. http://dx.doi.org/10.7326/0003-4819-152-7-201004060-00007.

Santos, F.C., Pacheco, J.M., Lenaerts, T., 2006. Evolutionary dynamics of social dilemmas in structured heterogeneous populations. Proc. Natl. Acad. Sci. 103 (9), 3490–3494.

Shakarian, P., Roos, P., Johnson, A., 2012. A review of evolutionary graph theory with applications to game theory. Biosystems 107 (2), 66–80.

Sharma, N., Traulsen, A., 2022. Suppressors of fixation can increase average fitness beyond amplifiers of selection. Proc. Natl. Acad. Sci. 119 (37), e2205424119.

Thain, D., Tannenbaum, T., Livny, M., 2005. Distributed computing in practice: The Condor experience. Concurr. Comput.: Pract. Exper. 17 (2–4), 323–356. http://dx.doi.org/10.1002/cpe.938.

Tkadlec, J., Pavlogiannis, A., Chatterjee, K., Nowak, M.A., 2019. Population structure determines the tradeoff between fixation probability and fixation time. Commun. Biol. 2 (1), 138. http://dx.doi.org/10.1038/s42003-019-0373-y.

Wahlberg, N., Klemetti, T., Hanski, I., 2002. Dynamic populations in a dynamic landscape: The metapopulation structure of the marsh fritillary butterfly. Ecography 25 (2), 224–232.

Wright, S., 1943. Isolation by distance. Genetics 28 (2), 114.

Yagoobi, S., Traulsen, A., 2021. Fixation probabilities in network structured meta-populations. Sci. Rep. 11 (1), 1–9.

Yagoobi, S., Yousefi, H., Samani, K.A., 2018. Mutation-selection stationary distribution in structured populations. Phys. Rev. E 98 (4), 042301.